CHAPTER 8

SUMMARY AND CONCLUSION

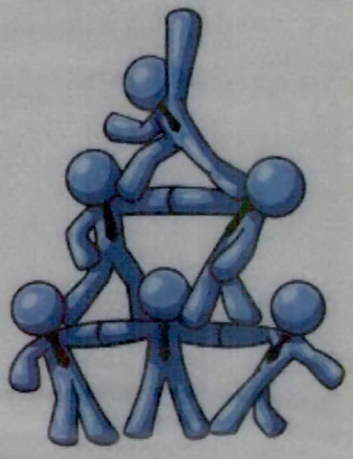

Liver fibrosis is the reversible wound healing response to a variety of chronic injurious events to the liver, induced by chronic viral hepatitis, iron or copper overload disease, certain autoimmune diseases, toxicity by certain drugs or chronic alcohol abuse and metabolic disorders, such as the metabolic syndrome. The disease is characterized by the deposition of excessive amounts of extracellular matrix (ECM) or "scar" tissues in the liver, which disturbs liver structure and functioning. In an advanced stage, the fibrotic process acquires a self-perpetuating character, and fibrosis will gradually progress into its end-stage called cirrhosis even when the injurious stimulus is removed. Finally, healthy liver cells are largely replaced by connective tissue. This remodeling of the liver parenchyma also results in impaired blood flow through the liver, which subsequently leads to portal hypertension and many secondary problems. In contrast to the early stages of the disease, when loss of functional liver parenchyma can still be compensated for by virtue of a functional over-capacity of the liver, liver function becomes de-compensated in the cirrhotic end-stage of the disease, ultimately leading to death. Liver transplantation is the ultimate treatment of advanced fibrosis but because of lack of liver donors, high costs and complexity of this therapy, there is a strong urge to establish alternative treatments.

The overall prevalence of cirrhosis in the United States is estimated at 360 per 100,000 population, or 900,000 total patients, the large majority of who have chronic viral hepatitis or alcoholic liver disease. Cirrhosis affects hundreds of millions of patients worldwide. In the US, it is the most common non-neoplastic cause of death among hepatobiliary and digestive diseases, accounting for approximately 30,000 deaths per year. In addition 10,000 deaths occur due to liver cancer, the majority of which arise in cirrhotic livers, with the mortality rate steadily rising.

Hepatic fibrosis has evolved in the past 20 years from a pure laboratory discipline to an area of great bedside relevance to practicing hepatologists. This evolution reflects growing awareness not only of the molecular underpinnings of fibrosis, but also of its natural history and methods of detection in chronic liver disease. These advances have culminated in clear evidence that cirrhosis can be reversible, and in realistic expectations that effective antifibrotic therapy will significantly alter the management and prognosis of patients with liver disease.

Within the fibrotic liver, activated hepatic stellate cells (HSC) produce excessive amounts of extracellular matrix proteins, which are the building blocks of the connective tissue. Under the influence of fibrogenic stimuli derived from damaged hepatocytes, activated Kupffer cells and liver endothelial cells, HSC transdifferentiate from a quiescent cell type into a cell with a myofibroblast-like phenotype. During fibrosis, the number of active fibrogenic cells in the liver also dramatically increases, mainly as a result of an increased local proliferation of HSC and is typically preceded by an influx of inflammatory cells and associated with subsequent ECM accumulation. Because the prolification process plays an important role in the progression of the disease, inhibiting HSC proliferation could be a relevant strategy to inhibit liver fibrosis in a pharmacological manner.

The best anti-fibrogenic treatment would be represented by any strategy able to eliminate the primary cause of parenchymal damage, metabolic overload or excessive oxidative stress. Once this primary requirement is fulfilled, the association with an anti-fibrogenic drug would be relevant for stabilizing the cure and favor optimal remodeling. Since the fibrogenic process is in its essence a compensatory phenomenon aimed at maintaining sufficient tissue continuity and cohesion in the presence of continuous microscopic parenchymal collapse, it would be erroneous to attempt to cure fibrogenic chronic liver diseases (CLDs) only with anti-fibrogenic drugs once some effective compounds will become available for clinical use.

So far no effective treatment has been established other than removal of primary cause of the disease and liver transplantation for severe fibrosis. Therefore, research is being carried out on therapeutic agents who inhibit activation and proliferation of HSC, reduce ECM production by HSC, neutralize HSC contractile responses or stimulate HSC apoptosis.

Expression of PPAR-γ by Rosiglitazone (RGZ) inhibited PDGF-induced proliferation and migration of vascular smooth muscle cells. The level of PPAR-γ and its trans-activating activity were diminished during HSC activation in vitro, whereas NF-κB and activator protein- 1 (AP-1) activities were increased. PPAR-γ ligands (RGZ) inhibited cell proliferation and collagen- α1(I) expression in primary HSC (3–4 days). The dramatic reduction in the abundance of PPAR-γ results in a significant decline in response to exogenous PPAR-γ ligands in activated HSC. These are suggestive of a

potential therapeutic value of PPAR-γ ligands in treatment of liver fibrosis if the expression of PPAR-γ can be induced in activated HSC.

The rennin–angiotensin system (RAS) plays an important role in the pathogenesis of organ fibrosis. Blockade of the RAS by angiotensin converting enzyme (ACE) inhibitors or by AT1 antagonists [Candesartan (CDS)] has been shown to improve the progression of organ fibrosis. Ang II induces proliferation and contraction of human HSCs, and TGF-b expression in rat HSCs, which are mainly mediated by AT1 receptors, and that ACE inhibitors or AT1 antagonists (CDS) attenuate the progression of liver fibrosis in vivo. These are suggestive that Ang II and RAS might play an important role in the pathogenesis of liver fibrosis.

One of the perceived benefits of liposomes as a drug carrier is based on their ability to alter favorably the pharmacokinetic profile of the encapsulated species and thus provide selective and prolonged pharmacological effects at these sites of administration. The resulting decrease in the frequency of drug dosing will significantly improve the quality of life for patients and at the same time reduce healthcare cost. Liposomes have tremendous potential as a carrier because they are nontoxic, non-immunogenic, and biodegradable and have a high loading capacity for a variety of therapeutic agents and have been investigated for long period of time.

Conventional liposomes are often less effective due to lack of the target specificity. In addition, rapid elimination and widespread distribution into targeted organs and tissues requires the administration of a drug in large quantities, which is not economical and often results in undesirable toxicity. Thus, drug targeting has evolved as the most desirable but elusive goal in drug delivery science. It can potentially increase efficacy and reduce toxicity of new and pre-existing drugs by altering their pharmacokinetics and biodistribution and restricting the action of drugs to the treated tissue. Hence, the major challenge is to design drug delivery strategies that deliver the therapeutic agents to the desired intracellular targets based on ability to understand, utilize, modify and exploit membrane trafficking pathways. Conjugating cell specific ligands to liposomes makes them target specific delivery system.

Mannose 6-phosphate receptor are over expressed on the surface of HSCs during liver fibrosis. Mannose 6-phosphate modified human serum albumin (M6P-HSA) is selective to M6P/IGF II receptor and thus accumulates in activated HSCs of fibrotic

liver. M6P-HSA conjugated liposomes can be used as HSCs selective carrier of antifibrotic drugs to improve the efficacy of drugs at the same time to reduce their adverse effects. Liposomes with bioactive lipid dilinoleoylphosphatidylcholine (DLPC) into the membrane as a major constituent act as a bioactive drug carrier which can deliver drugs and simultaneously have beneficial antifibrotic effects.

The objectives of this investigation were to develop liposomal formulation by thin film hydration method and optimized for drug: total lipid ratio, Phospholipid: cholesterol ratio and total solid: hydration medium ratio to maximize the percentage drug entrapment (PDE) and to minimize percentage reduction (PR) in PDE after 10 days by 3^3 full factorial design, to synthesize and characterize M6P-HSA and surface conjugation of optimized liposomal formulations. It was also an objective to assess release kinetics of developed formulations by performing *in vitro* drug diffusion studies and also to evaluate *in-vivo* pharmacokinetic and pharmacodynamic properties of prepared formulation in carbon tetrachloride (CCL_4) induced rat liver fibrosis model for exploitation of the findings of the studies in developing relevant product for effective treatment of liver fibrosis.

The developed spectroscopic determination methods of RGZ were based on the zero order UV spectra giving maxima at 311.8 nm in methanol (for estimation of RGZ in formulation) and at 313.8 nm in diffusion medium and found to be linear in the rage of 10-70 µg/mL having r^2 value of 1.0000 and 0.9995 respectively and had high accuracy and precision.

The developed spectroscopic determination methods of CDS were based on the zero order UV spectra giving maxima at 304.8 nm in methanol (for estimation of CDS in formulation) and at 306.2 nm in diffusion medium and found to be linear in the rage of 5-80 µg/mL having r^2 value of 0.9998 and 0.9996 respectively and had high accuracy and precision.

The developed chromatographic method of RGZ in plasma was based on reversed-phase HPLC method with UV detection having mobile phase composition of 10mM sodium acetate (pH 5): acetonitrile: methanol (40:40:20, v/v/v) at a flow rate 1.0 $mL \cdot min^{-1}$. RGZ was detected at 245.0 nm and calibration plot was linear ($r^2 > 0.9996$) in the concentration range of 0.05-10 µg/mL and had high accuracy and precision.

The developed chromatographic method of CDS in plasma was based on reversed-phase HPLC method with UV detection having mobile phase composition of methanol: acetonitrile: 10mM sodium acetate pH 5 (74 : 16 : 10, v/v/v) (pH 2.5) at a flow rate 1.0 $mL \cdot min^{-1}$. CDS was detected at 260.0 nm and calibration plot was linear ($r^2 > 0.9997$) in the concentration range of 0.05-10 µg/mL and had high accuracy and precision.

The developed analytical methods for estimation of mannose (colorimetric), phosphorus (colorimetric), total protein (colorimetric), albumin in serum (colorimetric), globulin in serum (colorimetric), aspartate aminotransferase (AST) in serum (colorimetric), alanine aminotransferase (AST) in serum (colorimetric), hydroxyproline in tissue (colorimetric), hyaluronic acid in serum (ELISA), total bilirubin in serum (colorimetric) were found to be linear in analytical ranges and had higher accuracy and precision.

Liposomes containing RGZ and CDS were prepared by TFH technique using DLPC, HSPC, DSPE-COOH and CH. Process parameters such as organic solvent composition, solvent evaporation time, speed of rotation, hydration time and vacuum applied were optimized to obtain desired formulation characteristics. The size of liposomes was the reduced using successive extrusion through 1, 0.4, 0.2 and 0.1 µm polycarbonate membrane filter. Liposomal suspensions were then characterized for vesicle size, size distribution, zeta potential and encapsulation efficiency. The RGZ loaded and CDS loaded liposomal formulations were optimized using 3^3 factorial design by varying drug: lipid molar ratio (1:15, 1:20 and 1:25), lipid: cholesterol molar ratio (9:1, 8:2 and 7:3), and total solid content: volume of hydration media ratio (1:10, 1:12.5 and 1:15) at 3 different levels as low (-1), medium (0) and high (1), by keeping all other process and formulation parameter invariant, to maximize PDE and to minimize PR in PDE after 10 days kept at refrigerated condition.

RSM was applied to fit second order polynomial equations, obtained by multiple linear regression analysis (MLRA) approach. Statistical soundness of the full and reduced polynomial equations was established on the basis of ANOVA statistics.

Two dimensional contour plots and three dimensional response surface plots were established by varying levels of two factors and keeping the third factor at fixed levels

at a time. Optimized formulation was derived by specifying goal and importance to the formulation variables and response parameters.

For RGZ liposomes, the optimized batch (Drug: Lipid molar ratio = -0.02; Lipid: Cholesterol molar ratio = 0.40; Total solid content: Volume of hydration media = 0.02) showed PDE of 71.83 ± 0.683 and PR in PDE of 2.41 ± 0.081. P-value > 0.05 indicates the differences between predicted and experimental values are statistically insignificant. In checkpoint analysis higher r^2 values (0.9947 and 0.9995 for PDE and PR respectively) of the linear correlation plots suggest excellent goodness of fit and high predictive capability of RSM.

For CDS liposomes, the optimized batch (Drug: Lipid molar ratio = -0.35; Lipid: Cholesterol molar ratio = 0.60; Total solid content: Volume of hydration media = -1.00) showed PDE of 64.01 ± 0.772 and PR in PDE of 2.481 ± 0.076. P-value > 0.05 indicates the differences between predicted and experimental values are statistically insignificant. In checkpoint analysis higher r^2 values (0.9894 and 0.9965 for PDE and PR respectively) of the linear correlation plots suggest excellent goodness of fit and high predictive capability of RSM.

M6P-HSA was successfully synthesized, purified, characterized for protein content, number of M6P molecules and number of phosphate groups coupled to each HSA molecules. The prepared neoglycoprotein had 95.22 ± 1.74% of protein, 29.73 ± 1.21 numbers of M6P molecules and 31.28 ± 2.01 numbers of phosphate groups coupled to each HSA molecule. Prepared M6P-HSA was then successfully conjugated to optimized liposomes and successful conjugation was confirmed by FTIR spectroscopy, particle size and zeta-potential analysis.

The size of Liposomes was measured by dynamic light scattering with a Malvern Zetasizer. Increased particle size and zeta potential of liposomes substantiate conjugation of M6P-HSA to liposomes.

The structure of liposomes was examined by TEM before and after conjugation of M6P-HSA. Liposomes had spherical shape and unilamellar structure. The liposome membranes were clearly observable because the inner aqueous compartments were slightly darker than the surrounding perimeters. The size of liposomes varied from 70 nm to 130 nm with an average diameter of 92.37 ± 3.28 nm for RGZ unconjugated liposomes (figure 4.24a) and 96.45 ± 3.71 for CDS unconjugated liposomes (figure

4.25a). The size of liposomes varied from 120 nm to 160 nm with an average diameter of 135.1 ± 3.74 nm for RGZ M6P-HSA conjugated liposomes (figure 4.24b), and 139.5 ± 3.98 for CDS M6P-HSA conjugated liposomes (figure 4.25b) measured by laser diffraction using Malvern Zetasizer. Results obtained from both TEM study and laser diffraction are parallel to each other.

The liposomal suspensions were stabilized by lyophilization. Different cryoprotectants at various ratios and anti-adherent were evaluated. The lyophilized formulations were tested for particle size, zeta potential and percentage drug retention (PDR). With use of sucrose, lactose and mannitol as cryoprotectant particle size of liposomes was increased and zeta-potential was decreased significantly after lyophilization. With trehalose, the lyophilized liposomes formed fluffy and snow like voluminous cake. With trehalose as cryoprotectant, the lyophilized liposomes were redispersed easily and the increase in particle size and decrease in zeta-potential were not significant. Trehalose at a ratio of 1:5 was used (as no further improvement was observed at 1:10) as a cryoprotectant and 10 % (of total solid) of glycine as antiadherent for lyophilization of optimized batches of liposomes.

Differential Scanning Calorimetry (DSC) studies and X-ray Diffraction (XRD) studies were conducted for lyophilized batches of M6P-HSA conjugated liposomes. DSC curves of plain drugs and liposomal formulations suggest loss of drug crystallinity when drugs were loaded into the liposomes. X-ray diffractograms showed less intensity of peaks corresponding to liposomal formulation than plain drug suggesting loss of drug crystallinity when drug was loaded into the liposomes.

To maintain sink condition, 50 ml of diffusion medium (50 mM Hydroxypropyl-beta-cyclodextrin, 20 mM HEPES, pH 7.4) for RGZ and 50 ml of diffusion medium (100 mM Hydroxypropyl-beta-cyclodextrin, 20 mM HEPES, pH 7.4) for CDS were selected and kept in receptor compartment with constant stirring at 37° ± 0.5°C.

Cumulative percent drug diffusion was plotted against time (t). The *in-vitro* release data obtained were fitted into equations for the zero-order, first- order and higuchi release models. The non-linearity of the graph for unconjugated and conjugated liposomal formulations suggests that the diffusion pattern does not follow zero order kinetics of release. Highest regression coefficient value for the first order model was found for plain drugs [RGZ (0.9833); CDS (0.9827)] and for the higuchi model for

both the unconjugated [RGZ (0.9768); CDS (0.9789)] and M6P-HSA conjugatd liposomes [RGZ (0.9796); CDS (0.9818)], indicating diffusion to be the predominant mechanism of drug release in both the cases of liposomes. In case of RGZ, Mean steady state flux were 37.78, 6.89 and 6.48 for plain drug, unconjugated liposomes and M6P-HSA conjugatd liposomes respectively. In case of CDS, mean steady state flux were 30.66, 6.58 and 6.08 for plain drug, unconjugated liposomes and M6P-HSA conjugatd liposomes respectively.

Comparative stability studies were carried out of the potential liposomal formulations at accelerated condition (25°C ± 2°C, 60% RH ± 5% RH) for six months and at long-term conditions (5°C ± 3°C) up to twelve months. The liposomal formulations were examined visually for the evidence of discoloration. The content of the vial are tested for percentage drug retention (PDR), particle size, zeta-potential, assay and water content. No significant differences were found in all above mentioned parameters at both conditions.

Experimental liver fibrosis was developed, using an established protocol with slight modification, that involved intraperitoneal (i.p.) injections CCl_4 premixed with olive oil. After 8 weeks from the first injection of CCl_4, animals were sacrificed and parameters such as serum albumin (ALB), serum globulin (GLB), total protein, serum alanine amino-transferase (ALT), serum glutamate-pyruvate transaminase (AST), blood glucose, serum levels of hyaluronic acid, liver coefficient, liver fibrosis grade, hydroxyproline content of the liver tissue were measured. After sacrificing the animals, liver was immediately removed and washed with saline and fixed in 10% buffered formalin. The fixed tissues were embedded in paraffin, five μm thick serial sections were cut and then processed for hematoxylin and eosin (H&E), masson's trichrome, picro-sirius red and α-SMA staining according to standard procedures.

The physical parameters such as liver fibrosis grade and liver coefficient were significantly increased in the CCl_4 induced liver fibrosis group rats compared to control group. Biochemical parameters such as serum AST, ALT, total bilirubin, hyaluronic acid and liver hydroxyproline were significantly increased and serum albumin/globulin ratio was significantly reduced in fibrotic rats. Plain RGZ, plain CDS, RGZ as well as CDS loaded unconjugated liposome treated groups demonstrated very modest improvement in the physical and biochemical parameters.

Blank conjugated liposomes displayed slight improvement due to presence of bioactive lipid DLPC and targeting ability. Most improvement, i.e. 13 to 70% in physical and biological parameters, had been observed in RGZ loaded conjugated liposome and CDS loaded conjugated liposome treated animal groups. Fibrosis grade, liver coefficient, serum AST, ALT, total bilirubin, hyaluronic acid and liver hydroxyproline content were significantly reduced and serum albumin/globulin ratio was increased as compared to CCl_4 induced liver fibrosis model group rats as given in the table 7.1 and 7.2. Significant reduction in serum glucose level was observed for plain RGZ and RGZ loaded unconjugated liposomes but no significant change was observed for RGZ loaded M6P-HSA conjugated liposomes suggesting very minimal or no systemic side effects of RGZ when given in conjugated liposomes.

Sections taken from rats of the control group showed normal architecture and have very less collagen and α-SMA deposition. The tissue architecture was very much disordered in the sections from fibrosis model group. Collagen and α-SMA depositions were also much more extensive. Here also the improvement was in order of RGZ loaded conjugated liposome = CDS loaded conjugated liposome > blank conjugated liposomes > RGZ loaded unconjugated liposomes = CDS loaded unconjugated liposomes > plain RGZ = plain CDS.

After 8 weeks of first injection of CCl_4, rats were injected with drug loaded M6P-HSA conjugated liposomes, drug loaded unconjugated liposomes and plain drug. Blood samples were collected at different time intervals of 5, 10, 20, 30 min and 1 h after injection. Total amount of the drug present in serum at each time point was measured by HPLC method. Similar experiments were performed for conjugated liposomes in rats pre-injected with M6P-HSA or HSA at the dose of 13 mg/kg of body weight (intravenous) 5 min before the injection of drug loaded M6P-HSA conjugated liposomes. From the obtained serum concentration data, the pharmacokinetic parameters were derived for each group.

After 10 min of injection, almost 87.91% of the injected dose for RGZ loaded conjugated liposomes cleared from the blood circulation, which was 2.61 folds higher than RGZ unconjugated liposomes and 4.93 folds higher than plain RGZ. After one hour, only 3.12% of the injected dose was present in the blood for RGZ loaded

conjugated liposomes, which were 11.03 and 24.27 folds lower than RGZ loaded unconjugated liposomes and plain RGZ respectively.

After 10 min of injection, almost 88.27% of the injected dose for CDS loaded conjugated liposomes cleared from the blood circulation, which was 2.57 folds higher than CDS unconjugated liposomes and 5.23 folds higher than plain CDS. After one hour, only 3.53% of the injected dose was present in the blood for CDS loaded conjugated liposomes, which were 10.49 and 21.35 folds lower than CDS loaded unconjugated liposomes and plain CDS respectively. Prior injection of M6P-HSA significantly reduced the blood clearance and increased half life of RGZ loaded and CDS loaded conjugated liposomes.

After one hour of injection, liver, spleen, kidneys, lungs and heart were excised, made free from any adhering tissues, weighed and drug content was measured in each organ by HPLC method after extraction. Almost 74.23 ± 1.55% of the injected dose had been taken up by the liver for the RGZ loaded conjugated liposomes which was 1.94 and 12.60 folds higher than RGZ loaded unconjugated liposomes and plain RGZ respectively. Very minuscule that is 4.82 ± 0.69%, 1.94 ± 0.47%, 3.61 ± 0.61% and 0.94 ± 0.2% of the injected dose had been taken up by the spleen, kidneys, lungs and heart respectively for the RGZ loaded conjugated liposomes. Amount taken up by the spleen, kidneys, lungs and heart was 2.08, 1.46, 1.08 and 1.18 folds more for RGZ loaded unconjugated liposomes and 1.10, 1.55, 0.56 and 1.43 folds more for plain drug than RGZ loaded conjugated liposomes.

Almost 73.97 ± 1.67% of the injected dose had been taken up by the liver for the CDS loaded conjugated liposomes which was 2.05 and 12.23 folds higher than CDS loaded unconjugated liposomes and plain CDS respectively. Very minuscule that is 4.94 ± 0.71%, 1.76 ± 0.43%, 3.57 ± 0.60% and 0.91 ± 0.19% of the injected dose had been taken up by the spleen, kidneys, lungs and heart respectively for the CDS loaded conjugated liposomes. Amount taken up by the spleen, kidneys, lungs and heart was 2.00, 1.44, 1.11 and 1.29 folds more for CDS loaded unconjugated liposomes and 1.07, 1.84, 0.61 and 1.34 folds more for plain drug than CDS loaded conjugated liposomes. Prior injection of M6P-HSA significantly reduced accumulation of RGZ and CDS in liver that is 1.60 and 1.61 folds lower than RGZ loaded conjugated liposomes and CDS loaded conjugated liposomes respectively.

Under this investigation, rosiglitazone and candesartan encapsulated liposomes were successfully prepared using thin film hydration technique. Particle size of the drug loaded liposomes was reduced by successive extrusion. Liposomal formulations were optimized using 3^3 full factorial design to maximize drug entrapment and to minimize percentage reduction in drug entrapment after 10 days kept at refrigerated condition. The experimental design and the derived polynomial equation for the optimization of liposomal formulation were validated for their utility by performing check point analysis. Optimized formulation was derived by specifying goal and importance to the formulation variables and response parameters. M6P-HSA was fruitfully synthesized and characterized. Prepared M6P-HSA was conjugated to optimized liposomes to impart ability to target hepatic stellate cells mainly responsible for liver fibrosis.

The characterization of conjugated liposomes demonstrated spherical shape, unilamellar structure and small particle size (< 200nm, even after lyophilization using trehalose as cryoprotectant) suitable for intravenous administration. Both drugs lost their crystallinity when loaded into the liposomes.

All these observations lead us to the conclusion that liposomal drug delivery has a greater potential for sustained diffusion of drug. Drug diffusion from liposomal formulations obeys Higuchi's diffusion controlled model and the diffusion rate is close to first order kinetics. The diffusion rate depends upon the physicochemical property, concentration of drug within the liposomes and the composition of the liposomal membrane. Hence by altering the composition of the liposomal membrane, different loading dose followed by maintenance dose can be achieved. Moreover the drug release been slower, it provides prolonged therapeutic response and also helps in prevention of development of drug resistance.

The decrease in drug assay, percentage drug retained, and zeta-potential and increase in water content, particle size were observed at accelerated condition (25°C ± 2°C, 60% RH ± 5% RH) for six months and at long-term conditions (5°C ± 3°C) up to twelve months for both RGZ and CDS liposomal formulation but the changes were statistically insignificant. Hence, both the formulations were considered as stable.

Due to lake of targeting knack plain RGZ, plain CDS, RGZ as well as CDS loaded unconjugated liposome treated groups demonstrated very modest improvement in the physical and biochemical parameters. Blank conjugated liposomes displayed slight

improvement due to presence of bioactive lipid DLPC and targeting ability. Most improvement had been observed in RGZ loaded conjugated liposome and CDS loaded conjugated liposome treated animal groups. Serum glucose level estimation studied suggests very minimal or no systemic side effects of RGZ when given in conjugated liposomes.

The histopathological studies suggests that improvement was in order of RGZ loaded conjugated liposome = CDS loaded conjugated liposome > blank conjugated liposomes > RGZ loaded unconjugated liposomes = CDS loaded unconjugated liposomes > plain RGZ = plain CDS.

M6P-HSA conjugated liposomes were rapidly taken up by the target cells as compared to unconjugated liposomes and plain drug. Prior injection of M6P-HSA significantly reduced the blood clearance and increased half life of RGZ loaded and CDS loaded conjugated liposomes, which confirms target specificity of M6P-HSA conjugated liposomes.

After one hour of injection, in case of M6P-HSA conjugated liposomes, much higher percentage of injected dose had been taken up by liver as compared to unconjugated liposomes and plain drug. In comparison to unconjugated liposomes and plain drug, very minuscule percentage of the injected dose had been taken up by the spleen, kidneys, lungs and heart for the RGZ loaded conjugated liposomes. Prior injection of M6P-HSA significantly reduced accumulation of RGZ and CDS in liver which confirms target specificity of M6P-HSA conjugated liposomes.

To conclude, M6P-HSA functionalized liposome based drug delivery systems of different class of drugs, such as PPAR gamma agonist (rosiglitazone) and angiotensin II receptor antagonist (candesartan), were successfully prepared, optimized and assessed pharmacokinetically and pharmacodynamically in suitable animal model. Drugs were selected on the basis of their possible potential efficacy in treatment of liver fibrosis but are not in use due to associated side effects. Pharmacokinetic data of the conjugated liposomes support effective liver targeting after intravenous administration. Pharmacodynamic studies, conducted in terms of biochemical and histopathological assessment, suggest potential application of drug loaded M6P-HSA conjugated liposomes in treating liver fibrosis which otherwise do not have any treatment except liver transplant, antioxidant therapy and vitamin supplements. The

studies of these investigations, support target specific exposure of drugs for prolonged period and reversal of liver fibrosis in experimental animal model. However, more extensive animal experimentation, on at least two more animal species, in terms of therapeutic efficacy and side effects are necessary to take up findings to clinical evaluation and use. This study provides a thinking which may result in development of product which can provide cure or at least prevention to this progressive disease necessitating liver transplant.